

# Quantitative Scoring of Muscle Involvement in MRI of Neuromuscular Diseases

M. E. Fantacci<sup>1,2</sup>, G. Astrea<sup>3</sup>, R. Battini<sup>3</sup>, A. Retico<sup>2</sup>, C. Sottocornola<sup>1,2</sup> and M. Tosetti<sup>3</sup>

<sup>1</sup>Physics Department, Pisa University, Largo Pontecorvo 3, Pisa, Italy

<sup>2</sup>Pisa Section of INFN, Pisa, Italy

<sup>3</sup>Stella Maris Scientific Institute, Calambrone, Pisa, Italy

**Keywords:** Muscle MRI, Neuromuscular Diseases, Muscle Segmentation.

**Abstract:** An automated method to evaluate the fat infiltration in tissues has been developed and applied to images of the human leg. The final aim is to obtain a quantitative evaluation of fat infiltration percentage and to relate it to the grade of muscle impairment in subjects affected by Neuro-Muscular Diseases (NMD). Through a muscle segmentation algorithm on structural T1-weighted magnetic resonance images (MRIs), the estimated non-muscle percentage (eNMP) in the segmented muscle area has been evaluated in healthy subjects as a reference value. A semi-automated procedure allows extending the algorithm to MRIs of NMD patients. A strong correlation has been demonstrated between the eNMP index and the disease severity.

## 1 INTRODUCTION

Magnetic Resonance Imaging (MRI) is an extremely useful imaging method to carry out reliable and non-invasive clinical assessment and follow up of subjects affected by NeuroMuscular Diseases (NMD).

In particular, as MRI is able to detect muscle involvement and to reveal the severity of disease, it is already used also in pediatric protocols for diagnostic study of NMD (Mercuri, 2002).

However, the interpretation of muscle MRI data and the assessment of NMD severity is currently carried out only visually by expert neurologists; software tools for automated quantitative analysis of muscle MRI have not yet been developed and provided in clinical diagnostic protocols. Standardization procedures and quantitative methods could be very useful instruments to optimize the muscle MRI diagnostic performance.

Recently the muscle fat fraction (MFF) has been evaluated (Gaeta, 2011; Gaeta, 2012), relying on the dual-echo dual-flip-angle spoiled gradient-recalled acquisition in the steady state (SPGR) magnetic resonance (MR) imaging technique. The muscle biopsy has been used in that case as reference standard.

A quantitative assessment has been made with Dixon method (Dixon, 1984) to highlight significant

increase in fat fraction in longitudinal studies (Willis, 2013).

Quantitative 3-point Dixon method has been compared to qualitative radiological scoring, concluding that the qualitative method overestimates the fat fraction (Wokke, 2013). In all cases, manual segmentation of each single muscle, which is an extremely time consuming task and hardly reproducible across different experts, is needed to compute the fat fraction in each ROI. Attempts to automatize the segmentation of skeletal muscles on Dixon images have recently been introduced, e.g. the automated computation of the fat fraction thought the extraction of subcutaneous adipose tissue with parametric deformable models (Makrogiannis, 2012) and the segmentation of calf muscles through Random Walks with shape prior information (Baudin, 2012).

In this paper we present a method for automatic quantitative analysis of T1-weighted Spin Echo (T1w SE) MR images of the leg, based on algorithms for tissues segmentation and histograms analysis. This method has been assessed on the images of healthy volunteers with the extraction of information used as reference standard in the analysis of the images of NMD patients in order to obtain a quantification of their fatty infiltrations and to study its correlation with the grade of muscle impairment in the NMD pathology.

## 2 MATERIALS AND METHODS

### 2.1 Subjects

Sixteen NMD patients and ten healthy subjects (HS) were considered for this study.

Patients age ranges between 1 to 54 years. In our Institute clinical studies follow the ethical guidelines of our local ethics committee. Informed written parental consent was obtained before the enrollment in the study. As expected, any side effects from muscle MRI examination has not observed. This examination is now routinely performed and does not require the use of anesthetic in young children after the 6 or 7 years of age. Sometimes muscle MRI has been performed in children less 6 yrs of age following general anaesthesia when brain MRI has been also required for diagnostic investigation.

The Medical Research Council (MRC) scale was used to assess the weakness in lower limbs. Patients were stratified in the five classes listed below according to MRC scores and maximal functional motor achievement: class 1 asymptomatic, class 2 mild symptomatic, class 3 moderate symptomatic, class 4 severely symptomatic, class 5 non-ambulatory. All patients except one were ambulatory.

The MRI exams of NMD patients were acquired between 2011 and 2012 at the MR laboratory of IRCCS Stella Maris Institute (Pisa, Italy) with a 1.5T scanner MR Signa GE Medical Systems HdXT with a whole body TX-RX coil. The standard MR protocol consisted of a 2D axial T1-weighted Spin Echo sequence with acquisition matrix of 256 x 256, FOV = 44 cm x 44 cm, TE = 14 ms and TR = 540 ms. The resulting images have an in-plane resolution of 1.72 mm x 1.72 mm and 5 mm of slice thickness.

Only the scan of the proximal third of the thigh of each subject was taken into account for analysis. All images were qualitatively assessed for the presence/absence of fat infiltration by a pediatric neurologist expert in muscle MRI, using the Mercuri grading (Mercuri, 2002).

The MRI scans of the ten healthy volunteers (healthy subjects, HS) have been acquired with the same acquisition protocol to obtain the reference standard for the eNMP (estimated Non Muscle Percentage) index in the healthy condition.

### 2.2 Software Tools

MRI data were analyzed with the medical image processing and visualization tool MeVisLab (MeVis Medical Solutions AG and Fraunhofer MEVIS in

Bremen, Germany, <http://www.mevislab.de/>). It consists in an image-processing environment with a special focus on visualization and analysis of diagnostic images. It is structured in a modular framework, where algorithms for segmentation, registration and quantitative image analysis can be implemented. It is based on Python programming language and modular expandable C++ image processing libraries. The Insight Toolkit (ITK) and Visualization Toolkit (VTK) software are integrated; they are open-source, freely available software systems that support computer graphics, image processing, modeling techniques and advanced visualization applications.

### 2.3 Characterization of Healthy Subjects

The MRI data set of the ten healthy subjects was studied in order to make an automatic analysis of anatomical features such as geometry and signal intensity of muscle and fat tissues.

We introduced an original index, the eNMP index, to take into account the fraction of non-muscle tissues, which are present within the muscle area. More in details, considering as muscle area the geometric area defined on the MR image excluding the bone and the subcutaneous fat by means of a segmentation procedure, it is evident that in this area blood vessels, nerves, fat and connective tissue are still included. By the eNMP index, the percentage of any tissues different from muscle included in the delineated muscle area is taken into account. To the best of our knowledge this reference standard obtained in the analysis of healthy subjects has not previously been reported in the literature.

The basic idea of the whole analysis is to take advantage of the different signal intensity of muscle and fat in MR images. An example of thigh MR image is shown in Figure 1, where the main muscle districts, the subcutaneous fat and the femur bone are clearly visible.

#### 2.3.1 Image Histogram Analysis

The analysis has been performed on a particular 2D image of the thigh, i.e. a slice selected by the child neurologist, where all the muscle sectors are clearly visible (at about half thigh length). It starts with a multiple Gaussian fit of the histogram of the image intensity values. Assuming that voxels values which are respectively part of muscle and fat tissue follow Gaussian distributions, a process of curve fitting has been executed in each histogram by using a least

squares fit method to find the mean and standard deviation values of subcutaneous fat and muscle distributions.

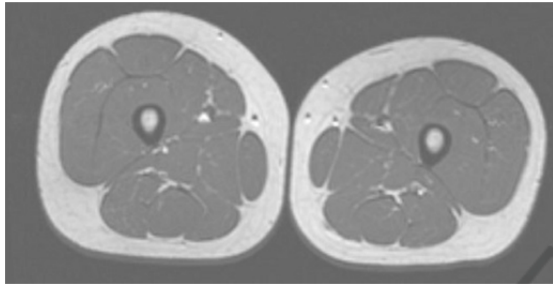


Figure 1: An axial T1-weighted MR image through the middle thigh of a healthy subject acquired with a 1.5 T MRI scanner.

The ratio between the fitted subcutaneous fat and muscle peaks ( $\mu_{\square}$  and  $\mu_{\text{F}}$ ) has been computed for all subjects and averaged, thus generating a standard reference measure of the ratio ( $R = \mu_{\text{F}}/\mu_{\square}$ ) of the intensity values of fat and muscle.

The ratio between the fitted subcutaneous fat and muscle peaks ( $\mu_{\square}$  and  $\mu_{\text{F}}$ ) has been computed for all subject and averaged, thus generating a standard reference measure of the ratio ( $R = \mu_{\text{F}}/\mu_{\square}$ ) of the intensity values of fat and muscle.

### 2.3.2 Muscle Area Segmentation

In the following step an automatic segmentation method has been performed in order to isolate muscle tissue from femur bone and subcutaneous fat; the objective was to quantify the percentage of voxels of non-muscular tissue as blood vessels, nerves and connective tissue present in muscular districts present in muscular district.

The automatic segmentation algorithm has been developed and implemented using a CSOIsoGenerator (Contour Segmentation Objects) module algorithm of the MeVisLab software package. The CSO library provides data structures and modules for an interactive or an automatic generation of contours in voxel images.

Furthermore, these contours can be analyzed, maintained, grouped and converted into a voxel image or a set of markers. The module CSOIsoGenerator generates iso-contours for a whole image at a fixed iso value: the input image is scanned by a marching-square algorithm that always produces closed CSOs. The border is treated as being always lower than the iso value and the CSOs can be interpolated by a linear interpolation scheme and/or smoothed by applying a spline

approximation. A Creation mode lets the user adjust which CSOs on one slice should be kept; if the mode is set to All, all CSOs are kept. If it is set to Largest, only the largest CSO (measured in number of seed points) on a slice is kept of the generating contours.

In our case, two different ISO contours are needed to isolate the muscle tissue from neighboring bone and subcutaneous fat. Within the segmented muscle area, also non-muscle components are present, including fat, connective tissue, nerves and blood vessels.

### 2.3.3 ENMP Index Evaluation

Allowing that the muscle tissue shows intensity values are in the  $\mu_{\text{M}} \pm 3\sigma$  range, where  $\mu_{\text{M}}$  is the fitted central of the muscle peak in the intensity histogram of each subject and  $\sigma$  is the standard deviation according to our Gaussian distribution assumption.

The eNMP has thus been computed (1) as the ratio of non-muscle components in the segmented muscle area:

$$\text{eNMP} = \frac{\sum_i n_i |(|I_i - \mu_{\text{M}}| > +3\sigma)}{\sum_i n_i |(|I_i - \mu_{\text{M}}| \leq +3\sigma)} \quad \forall i \in M \quad (1)$$

where  $n_i$  is the number of voxels with intensity  $I_i$  and  $i$  runs on all voxels belonging to the mask  $M$ , i.e. the muscle mask identified with the iso-contour based segmentation algorithm.

The eNMP index has been evaluated for all HC subjects and its average value constitutes the reference standard for the healthy population.

## 2.4 Analysis of NMD Patients

The evaluation of the eNMP has been carried out also on NMD subjects with the final aim to correlate it with the grade of muscle impairment in the NMD pathology.

In this case it is unfortunately very difficult to discriminate the subcutaneous fat from the fat infiltrated in the muscle with an automated segmentation procedure, as shown in the two example of Figure 2. For this reason, an expert child neurologist was asked to interactively draw the manual subcutaneous fat delineation contour, thus defining the muscle masks also in case of NMD subjects. Once verified the validity of the method, in the near future it may be possible an automatic segmentation of the muscle area by means of a three-dimensional image analysis based on innovative image processing methods developed for very noisy image segmentation as, for example

virtual ants based models (Cerello, 2010). Taking into account the known ratio  $R$  between the intensity values of fat and muscle in our images, and measuring through a Gaussian fit the average value of the fat ( $\mu_f$ ) in the MRI image of a NMD patient, the corresponding  $\mu_m$  has been obtained. The eNMP index has thus been evaluated also for NMD subjects and is available for correlation with the NMD severity.

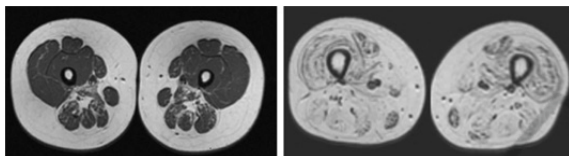


Figure 2: Two examples of axial image of thighs in NMD patients. On the left a NMD patient with a low-grade MRC score (mild symptomatic) and mild involvement of thigh muscles in the posterior compartment. On the right a second patient with a high-grade MRC score (severely symptomatic) and massive fat infiltration of all the thigh's muscles with only minimal preservation.

### 3 RESULTS

To compute the eNMP index, first of all the  $\mu_m$ ,  $\sigma_m$ ,  $\mu_f$  and  $\sigma_f$  values were obtained through a multiple Gaussian fit on the image histogram of the ten healthy subjects. The values obtained are reported in Table 1, where also the ratio  $R = \mu_f/\mu_m$  is shown together with the estimated error on these quantities. The average ratio results  $R^M = 3.4 \pm 0.3$ . This quantity has been used as a reference standard in the analysis of NMD patients. The eNMP index computed for each HS is also reported in Table 1. It can be noticed that the eNMP indices computed on HS never exceeded the threshold of 7%.

Table 1: The  $\mu_m$ ,  $\sigma_m$ ,  $\mu_f$  and  $\sigma_f$  values obtained through a Gaussian fit on the image histogram for each HS are reported. The ratio  $R = \mu_f/\mu_m$  is also shown. The last column reports the eNMP index obtained of each HS.

ID	$\mu_m$	$\sigma_m$	$\mu_f$	$\sigma_f$	R	eNMP
HS1	174.7	27.2	601.0	93.7	$3.4 \pm 0.8$	6.3%
HS2	162.3	25.8	548.0	91.4	$3.4 \pm 0.8$	5.1%
HS3	165.2	14.3	550.1	121.0	$3.3 \pm 0.9$	3.5%
HS4	146.6	25.0	470.6	109.5	$3.2 \pm 0.9$	6.2%
HS5	170.1	24.0	571.9	125.5	$3.4 \pm 0.9$	6.2%
HS6	177.3	30.6	615.8	89.6	$3.5 \pm 0.8$	6.6%
HS7	187.0	42.8	694.0	108.3	$3.7 \pm 1.0$	4.4%
HS8	164.7	30.4	542.0	114.1	$3.3 \pm 0.9$	6.5%
HS9	182.5	32.4	670.1	107.8	$3.7 \pm 0.9$	4.2%
HS10	189.6	28.4	669.4	87.5	$3.5 \pm 0.7$	6.3%

In the segmentation step to isolate muscle tissue from femur bone and subcutaneous fat the input image has been scanned by a marching-square algorithm that produces closed contour segmentation objects. The largest contour defines the boundary between the muscle and the surrounding subcutaneous fat, whereas the smaller defines the boundary between the muscle and the femur bone, as shown in Figure 3.

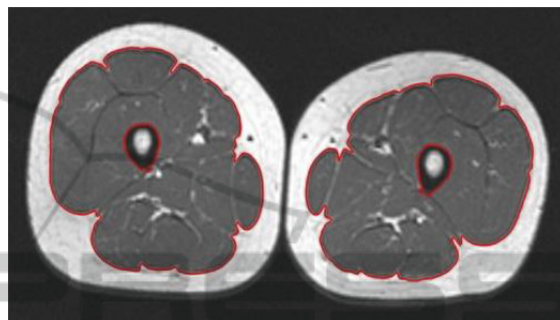


Figure 3: Example of automatic segmentation of femur bone and muscular district in a HC subject: the iso-contour generator module provides closed contours at fixed iso-values.

The muscle peak in the histograms of the images of NMD patients is far less evident, when not completely absent, whereas the fat peak is higher due to fat replacement in muscular area. Only the  $\mu_f$  and  $\sigma_f$  values have thus been extracted through a Gaussian fit from the histogram of the images of NMD subjects and are reported in Table 2. The corresponding  $\mu_m$  and  $\sigma_m$  expected values have been obtained for each NMD subject according to the average coefficient  $R^M$  estimated in the analysis of HC subjects. The so obtained eNMP indices are also reported for the NMD subjects in Table 2. It can be noticed that the eNMP indices obtained on NMD subjects are generally higher with respect to the HC subjects. The eNMP indices we computed on NMD subjects have also shown a positive correlation with the grade of muscle impairment in NMD subjects as well as it was evaluated from a clinical point of view by means of the MRC scale and from an imaging point of view with a visually grading (Mercuri, 2002). In particular, a strong correlation has been found between the visually scored muscle involvement (Mercuri grading) and the quantitative eNMP index estimated on MR images. In Figure 4 the scatter plot of the Mercuri grading versus the eNMP index is reported.

As the correlation between muscle involvement and disease severity is known not to be a linear function, with small advance of fat infiltration being

weightier in the first categories with respect to the higher ones (i.e. in those patients mild symptomatic respect to those severely affected), the Spearman rank correlation coefficient has been estimated, obtaining  $\rho = 0.97$  ( $p < 10^{-5}$ ). This preliminary result is very interesting from an analytical point of view and seem in agreement with clinical experience, that shows some patients with a high degree of fat infiltration but with a more of less stable clinical progression. This trend can also be related to the different pathogenetic mechanisms underneath the different diseases.

Table 2: The  $\mu_f$  and  $\sigma_f$  values obtained through a Gaussian fit on the image histogram for each NMD subject are reported. The last column reports the eNMP index obtained for NMD subjects.

ID	$\mu_f$	$\sigma_f$	eNMP
NMD1	590.8	61.9	6.4%
NMD2	678.0	62.3	18.6%
NMD3	680.4	51.6	35.6%
NMD4	591.5	50.3	26.2%
NMD5	544.5	74.0	29.0%
NMD6	674.3	68.3	41.7%
NMD7	585.8	37.3	48.6%
NMD8	629.2	34.4	60.2%
NMD9	719.4	50.9	18.8%
NMD10	658.2	67.5	35.7%
NMD11	698.3	64.0	4.7%
NMD12	751.7	42.6	96.6%
NMD13	735.5	34.9	34.7%
NMD14	581.0	59.4	9.2%
NMD15	650.2	79.3	13.1%
NMD16	599.4	61.0	28.6%

#### 4 CONCLUSIONS

A totally automatic analysis of MR images of the thigh of healthy subjects has been carried out, allowing the extraction of a reference standard useful for a semi-automatic evaluation of muscle involvement in NMD patients. Besides the strong correlation obtained between the Mercuri grading and the eNMP index, lower values of the eNMP involvement scores were attributable to patients with neurogenic alterations at muscle biopsy, correlated to less altered muscle structures, while higher eNMP values were found for the dystrophic patients, in correlation with their massive muscle architecture disruption. In view of realizing a fully automated system of quantitative analysis, the few morphological differences between subcutaneous fat

and fat infiltration in muscle may render ineffective the standard procedures of segmentation and the analysis of the two-dimensional MR images may not be sufficient for the automatic segmentation and quantitative analysis of the muscles in the pathological subjects. May therefore be necessary reformatting the volumes and making a three-dimensional analysis of three-dimensional images. Moreover, may have to be used innovative methods for pattern recognition such as the use of virtual ants and active contours methods driven by local/global histogram statistics. Then, such pattern recognition module devoted to the segmentation and 3D reconstruction of muscles area may be followed by a feature extraction tool which will be able to identify the characteristics which can indicate the presence of the pathology, both geometrical (i.e. muscular shapes and volumes) than related to the local signal intensities (i.e. presence of fibrosis or fat infiltration). In the last step these features will be used to train an artificial intelligence based classifier. Overall, these preliminary results show that a quantitative analysis of muscle MRI could be a promising instrument to quantify the patterns of fat infiltration in neuromuscular patients.

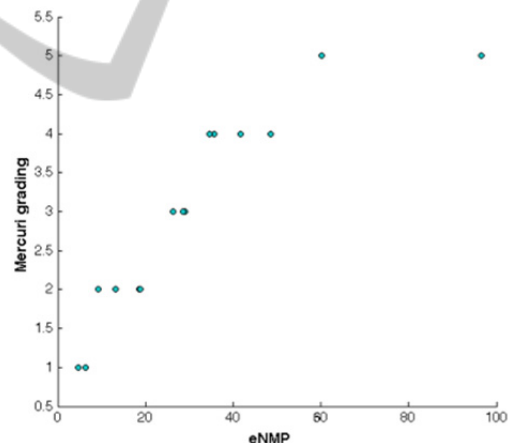


Figure 4: Scatter plot of the Mercuri grading versus the eNMP index obtained for each NMD patient.

#### REFERENCES

Baudin, P.Y. et al., 2012. Prior Knowledge, Random Walks and Human Skeletal Muscle Segmentation. *Lecture Notes in Computer Science* 7510:569-576.

Cerello, P. et al., 2010. 3-D object segmentation using ant colonies. *Pattern Recognition* 43(4):1476-1490.

Dixon, W.T., 1984. Simple proton spectroscopic imaging. *Radiology* 153:189-194.

Gaeta, M. et al., 2011. Muscle Fat Fraction in Neuromuscular Disorders: Dual-Echo Dual-Flip-

- Angle Spoiled Gradient-Recalled MR Imaging Technique for Quantification-A Feasibility Study. *Radiology* 259(2):487-494.
- Gaeta, M. et al., 2012. Muscle fat-fraction and mapping in Duchenne muscular dystrophy: evaluation of disease distribution and correlation with clinical assessments. *Skeletal Radiol* 41:955-961.
- Makrogiannis, S. et al., 2012. Automated quantification of muscle and fat in the thigh from water-, fat-, and nonsuppressed MR images. *J Magn Reson Imaging* 35(5):1152-61.
- Mercuri, E. et al., 2002. Clinical and imaging findings in six cases of congenital muscular dystrophy with rigid spine syndrome linked to chromosome 1p (RSMD1). *Neuromuscul Disord* 12:631-638.
- Willis, T.A. et al., 2013. Quantitative Muscle MRI as an Assessment Tool for Monitoring Disease Progression in LGMD2I: A Multicentre Longitudinal Study. *PLOS ONE* 8/8: e70993.
- Wokke B.H. et al., 2013. Comparison of dixon and T1-weighted MR methods to assess the degree of fat infiltration in duchenne muscular dystrophy patients. *J Magn Reson Imaging* 38(3):619-624.

